

Development of displacement- and frequency-noise-free interferometer in 3-D configuration for gravitational wave detection

Keiko Kokeyama*

*Graduate School of Humanities and Sciences, Ochanomizu University,
2-1-1, Otsuka, Bunkyo-ku, Tokyo 112-8610 Japan*

Shuichi Sato

Faculty of Engineering, Hosei University, 3-7-2, Kajino-cho, Koganei, Tokyo 184-8584 Japan

Atsushi Nishizawa

Graduate School of Human and Environmental Studies Kyoto University, Kyoto 606-8501 Japan

Seiji Kawamura

TAMA project, National Astronomical Observatory of Japan, 2-21-1, Mitaka, Osawa, Tokyo 181-8588 Japan

Yanbei Chen

Theoretical Astrophysics, California Institute of Technology, Pasadena, California 91125 USA

Akio Sugamoto

Ochanomizu University, 2-1-1, Otsuka, Bunkyo-ku, Tokyo 112-8610 Japan

The displacement- and frequency-noise-free interferometer (DFI) is a multiple laser interferometer array for gravitational wave detection free from both the displacement noise of optics and laser frequency noise. So far, partial experimental demonstrations of DFI have been done in 2-D table top experiments. In this paper, we report the complete demonstration of a 3-D DFI. The DFI consists of four Mach-Zehnder interferometers with four mirrors and two beamsplitters. The displacement noises both of mirrors and beamsplitters were suppressed by up to 40 dB. The non-vanishing DFI response to a gravitational wave was successfully confirmed using multiple electro-optic modulators and computing methods.

Gravitational waves are perturbations of the space-time curvature propagating across the universe at the speed of light. They propagate in space-time, extending a proper distance between test masses in one transverse direction, and shortening in the other, orthogonal direction. A laser-interferometric gravitational wave detector measures length differences between the optical components (test masses) caused by the gravitational wave effect. Various noise sources that limit the sensitivity of the detector must be removed to achieve the best sensitivity level, as the interferometers must detect the very tiny signals of length change. The sensitivities of the ground-based detectors are affected by seismic noise, thermal noise, radiation pressure noise, laser source noise (laser frequency and intensity noise), and shot noise. The seismic, thermal and radiation pressure noises can be categorized as *displacement noises* since the noise sources shake up the optics directly. These displacement noises limit the sensitivities especially in the low-frequency regime, which is the important region for the ground-based gravitational wave detectors, which target at several ten to several thousand Hz. Recently, the idea of a gravitational wave detector free from both the displacement noises of

the optics and the laser frequency noises at all frequencies has been proposed in Refs. [1, 2]. This technique exploits the fact that the gravitational wave effect on the laser light takes a form different from that of optics displacements. A signal combination which does not sense displacement- or frequency-noises but senses the gravitational wave contribution can be constructed when the array of N test masses consists of multiple interferometers under the condition that $N > d + 2$ (d is the number of spatial dimensions of the array). The next paper in the series of DFI papers, Ref. [3], suggested a 3-D DFI configuration consisting of four Mach-Zehnder interferometers (MZIs). This configuration is the most ideal of all DFI configurations so far proposed. A proof-of-principle experiment with a 2-D layout of a sub-part of this configuration was done in Ref. [4]. There, the cancellation of displacement noise from a folding mirror was demonstrated. However, the 2-D layout was half that of the 3-D DFI, and it cannot cancel the displacements of all the optics. In this paper, as a complete DFI system, we report the cancellation of the displacement both of the folding mirrors and beamsplitters while the gravitational-wave response is retained using the full 3-D DFI.

The 3-D DFI configuration is depicted in Fig. 1. Four MZIs with equal arm lengths compose the DFI. Let us denote by IFO_1 , IFO_2 , IFO_3 , and IFO_4 the four single MZIs drawn in orange (AC_1B-AD_1B), pink (AC_2B-AD_2B),

*Electronic address: keiko.kokeyama@nao.ac.jp

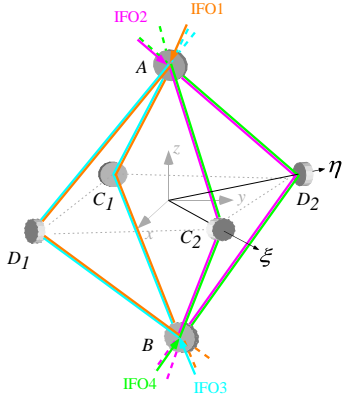


FIG. 1: (color online). Optical topology of 3-D DFI. The pairs of IFO₁ and IFO₃ and of IFO₂ and IFO₄ are counterpropagating to each other, constructing two bidirectional Mach-Zehnder interferometers (MZIs). Right and left bidirectional MZIs share the two beamsplitters. The length from A or B to each folding mirror is L .

light blue ($BC_1A - BD_1A$), and green ($BC_2A - BD_2A$) in Fig. 1. Each length between a beamsplitter and a mirror ($AC_1, AC_2, AD_1, AD_2, C_1B, C_2B, D_1B$, and D_2B) is assumed as L so that each interferometer is insensitive to laser frequency noise thanks to the equal arms. Two of the four interferometers are combined to construct one bidirectional MZI in which two beams are counterpropagating on the same path. As is discussed in Ref. [3], the DFI signal combination can be written as

$$\phi_{\text{DFI}} = (\phi_1 - \phi_3) - (\phi_2 - \phi_4) \quad (1)$$

where ϕ_j ($j = 1, 2, 3, 4$) are the phase signals of IFO _{j} . In Eq. (1), the combined signal of $(\phi_1 - \phi_3)$ is the output of the bidirectional MZI that is free from the displacements of C_1 and D_1 . Because the folding mirrors are at the midpoint of the arms, and the laser beams travel in both directions in the MZI, the phase variation due to the displacement of C_1 and D_1 arrives at each output port simultaneously. Therefore, in the frequency domain, IFO₁ and IFO₃ have identical transfer functions from the displacement of C_1 and D_1 to the signal ports, expressed as

$$H_1^{C_1, D_1}(\Omega) = H_3^{C_1, D_1}(\Omega) = e^{-iL\Omega/c}, \quad (2)$$

where c is the speed of light in vacuum, ω is the laser frequency and Ω the Fourier frequency of the displacement motion. The phase modulations due to the motions of the optics experience the same phase delay shown in Eq. (2) because the displacement sources are at the midpoint of the path. These identical responses to C_1 and D_1 can thus be removed by subtraction. Similarly, $(\phi_2 - \phi_4)$ is the signal of the other pair of bidirectional MZIs, and free from the displacements of C_2 and D_2 . Any signals that phase modulate the light and do not arise at the exact center of the path will not arrive simultaneously at the outputs, and thus will not be canceled by the bidi-

rectional MZIs. The beamsplitter displacements are removed by the combination of $(\phi_1 - \phi_2)$ in Eq. (1). Since the laser beams of IFO₁ and IFO₂ reach the two beamsplitters simultaneously, their responses to the beamsplitter motion are the same. Therefore, in the frequency domain, IFO₁ and IFO₂ have identical transfer functions from the displacement of A to the signal ports expressed as

$$H_1^A(\Omega) = H_2^A(\Omega) = e^{-2iL\Omega/c}. \quad (3)$$

The transfer functions of the displacement motion of beamsplitter B are $H_1^B(\Omega) = H_2^B(\Omega) = 1$ since the motions of B are just before the detection ports. Therefore the beamsplitter displacements can be eliminated by the combination of IFO₁ and IFO₂. Similarly, the combined signal of $(-\phi_3 + \phi_4)$ in Eq. (1) is free from the beamsplitter displacements. In practice, in addition to the transfer functions, extra phase delays should be considered that arise from the paths from the second beamsplitter to the signal analyzer via a photo detector and signal cables. These additional phase delays of each interferometer should be made equal or calibrated later, so as not to lose the balanced responses.

According to Ref. [3], the DFI signal responds to a gravitational wave with the transfer function,

$$H_{\text{GW}}(\Omega) = -\frac{i\omega}{\Omega} \left\{ (1 + 1/\sqrt{2})e^{-\frac{i\Omega L}{\sqrt{2}c}} \left(1 - e^{-\frac{2i\Omega L(1-1/\sqrt{2})}{c}}\right) - (1 - 1/\sqrt{2})e^{\frac{i\Omega L}{\sqrt{2}c}} \left(1 - e^{-\frac{2i\Omega L(1+1/\sqrt{2})}{c}}\right) \right\} \quad (4)$$

where Ω is the Fourier frequency of the gravitational wave and we assume the gravitational wave of $\eta - \xi$ polarization is coming along the z direction in Fig. 1. The 3-D DFI does not respond to DC gravitational waves because the response is degraded by the subtraction when the DFI signal is built by the four MZI signals. The DFI response is proportional to $(\Omega L/c)^2$ below the peak frequency. The peak frequency depends on the arm length L , e.g. when $L = 1$ m, the peak is at about 150 MHz. There have been several attempts to lower the effective frequency of DFI: Adding Fabry-Perot (FP) cavities to the 3-D DFI to increase the effective path lengths and lower the peak frequency; another method of displacement cancellation using one FP cavity [5, 6]. At this moment, our f^2 response at low frequencies is the best sensitivity that DFI configurations have achieved.

Figure. 2. shows the practical setup of our experiment. The laser source is a commercial solid-state Nd:YAG laser at 1064 nm. The light source is split into four by beamsplitters so as to provide the four incident beams for the four MZIs. As depicted in Fig. 2, IFO₂ and IFO₄ (denoted as higher interferometers) are lying over IFO₁ and IFO₃ (denoted as lower interferometers). The length L was chosen to be about 40 cm yielding peak frequency of about 370 MHz. There are two Faraday isolators before the lasers are sent to IFO₁ and IFO₂. They are used for extracting the signal of IFO₃ and IFO₄ (ports

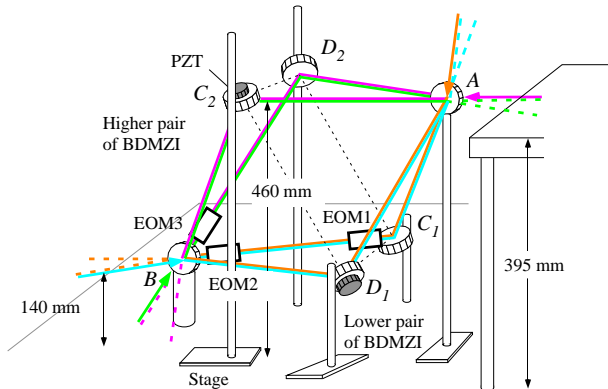


FIG. 2: (color online). Schematic of the experiment. The octahedron is pushed over sideways to be set up on an optical table. IFO₁ and IFO₃ comprise one bidirectional MZI, and so do IFO₂ and IFO₄. EOM1 simulates mirror C_1 displacement and EOM2 and EOM3 simulate beamsplitter B displacement.

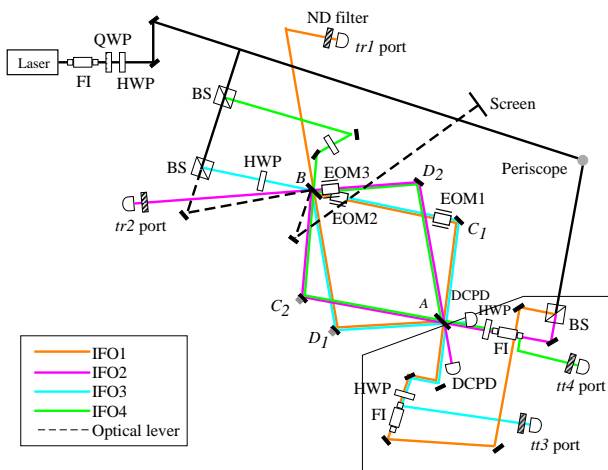


FIG. 3: (color online). The overhead view of the experimental setup. HWP: half wave plate, QWP: quarter wave plate, FI: Faraday isolator, BS: beamsplitter, DCPD: DC photo detector. There are four interferometers: IFO₁ ($A - C_1, D_1, -B$), IFO₂ ($A - C_2, D_2, -B$), IFO₃ ($B - C_1, D_1, -C$) and IFO₄ ($B - C_2, D_2, -A$). The black-dashed line indicates the optical lever method for the alignment of 3-D configuration.

$tt3$ and $tt4$ [8] exiting from the IFO₁ and IFO₂ inputs, respectively. The signals at ports $tr1$ and $tr2$ are directly detected by the photo detectors. The DC photo detectors (DCPD) are placed at ports $tr3$ and $tr4$ for extracting the control signals. The extracted DC signals are sent to the servo filters with static offsets, then sent to the piezoelectric transducers (PZTs) attached to mirrors D_1 and C_2 . D_1 and C_2 are controlled by signals giving the mid-fringe locking for the IFO₃ and IFO₄, respectively. Once IFO₃ is locked, IFO₁ is locked automatically. Likewise, locking IFO₂ automatically locks IFO₄. The control bandwidth of the two interferometers is about 1 kHz.

To align the four-interferometer system, we utilized an optical lever as shown in Fig. 3, using the fact that the lower and higher sets of bidirectional MZIs share their beamsplitters [7]. The positions and the angles of C_1 and of D_1 , and positions and angles of C_2 and of D_2 , inde-

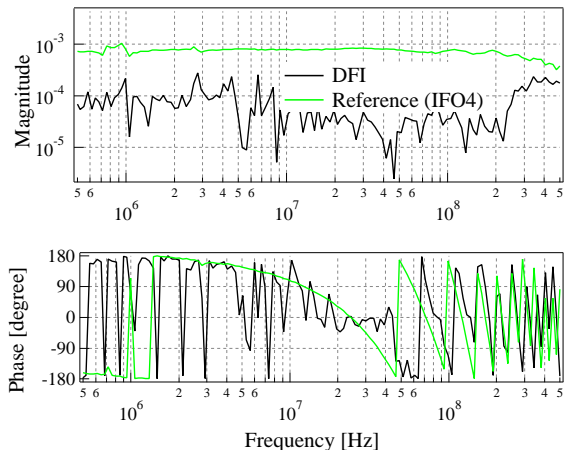


FIG. 4: (color online). The solid green line is the transfer function from EOM3 to $tt4$ as a reference, and the solid black line is the transfer function from EOM3 to the DFI signal. From one to two orders of magnitude of the cancellation were attained in the DFI signal.

pendently determine the position and angle of B for the alignment of the higher and lower interferometer, respectively. To make them compatible, the optical lever was utilized to monitor the angle of beamsplitter B . First, for the lower interferometer, the angle of B determined by C_1 and D_1 , is adjusted and monitored by the optical lever signal on the screen. For the higher interferometer, we then adjust the position and angle of B determined by C_2 and D_2 , is adjusted for the lower interferometer and displayed on the screen. And we adjust the positions and angles of C_2 , D_1 and A so that the two monitored marks on the screen come to exactly the same point which means the ideal angle of B . This method achieved an almost perfect contrast.

EOMs were utilized to create phase shifts to the laser light as simulated displacements of the optics because the interesting frequency, i.e., the response peak of the gravitational wave, is expected to be in the hundred-MHz region. To confirm the noise cancellation features of both mirror and beamsplitter, the three EOMs were driven; for simulating the displacement of mirror C_1 , EOM1 is placed at the center of the path BC_1A ; for simulating the displacements of beamsplitter B , EOM2 and EOM3 are placed close to B as beamsplitter B affects both the higher and lower interferometer. The EOMs were driven by swept-sine noise sources provided by the RF network analyzer (Agilent 4395A). The signals from the four MZIs are detected by four fast photo detectors (New Focus 1611) at ports $tr1, tr2, tt3$ and $tt4$. The optical gain imbalances between the four output signals are compensated by neutral density (ND) filters placed in front of each detector. The DFI signal is obtained by electrical summation of the four signals using electric power combiners. We adjusted the control polarity so that $tr1$ and $tr2$ have opposite sign so as to cancel by their summation.

The DFI response to a gravitational wave coming along

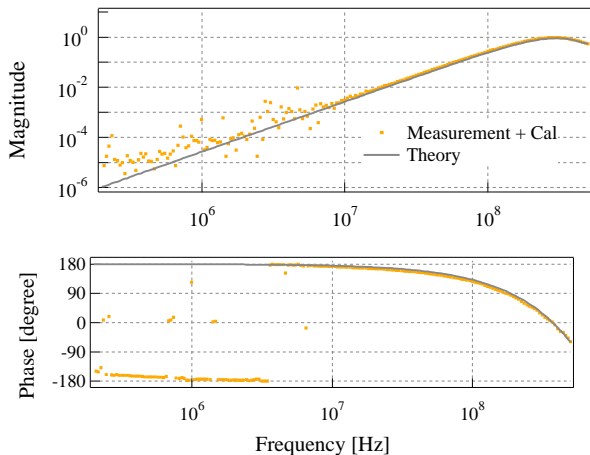


FIG. 5: (color online). The orange dots are the simulated DFI response to the gravitational wave obtained by being measured and computed, the gray solid line is the DFI response predicted by Eq. (4). The simulated response agreed with the theory.

z direction was demonstrated by multiple measurements and simulation. Ideally, the continuous phase variation should be applied on the entirety of the laser paths to simulate the gravitational-wave effect. However, only the part covered by the crystal causes a phase shift by an EOM. Therefore, the following procedure was adopted. We place an EOM in the laser path and measure the transfer function. Then we place the EOM at the next point and measure the transfer function, and so on. The measured data are summed up with proper phase delays that depend on the gravitational wave direction and the EOM position. For a gravitational wave coming along the AB axis, Eq. (4) can be approximated by the summation of the discrete phase shifts expressed as

$$H_{\text{GW}}(\Omega) \sim H_{\text{sum}}(\Omega) = \frac{\omega L}{cD} \left\{ e^{\frac{i\Omega L}{\sqrt{2}c}} \sum_{n=0}^{2D} e^{\frac{i\Omega L}{c} \frac{n}{D}} e^{-\frac{i\Omega L}{\sqrt{2}c} \frac{n}{D}} - e^{-\frac{i\Omega L}{\sqrt{2}c}} \sum_{n=0}^{2D} e^{\frac{i\Omega L}{c} \frac{n}{D}} e^{\frac{i\Omega L}{\sqrt{2}c} \frac{n}{D}} \right\} \quad (5)$$

under the condition $\Omega L/Dc \ll 1$. D is the resolution of the positions on the path of L where the phase shifts occur. Note that the straightforward way to produce

continuous phase shift is to insert EOMs along all laser path. However, that many EOMs covering laser paths will cause a serious reduction in interferometer contrast.

In the experiment, the phase shift part of $e^{i\Omega L n/Dc}$ in Eq. (5) was created practically by the EOM with the discrete resolution $D = 10$. For the first ten data, $n = 0 \dots 9$, an EOM was set in a respective position at nL/D from beamsplitter B , and the respective transfer functions were measured. Since we cannot put an EOM on C_1A , we compute the transfer function data for $n = 10 \dots 20$ applying proper phase delays to the data of $n = 9$. These data were summed with predicted phase delays due to the incident angle of the gravitational wave in accordance with Eq. (5), to construct the gravitational wave response.

The results for displacement-noise suppression are shown in Fig. 4. The solid black line is the transfer function from EOM1 to the DFI (combined) signal. The solid green line is the transfer function from EOM1 to a single MZI output (port $tt4$) as a reference. Comparing with these transfer functions, we can confirm that the DFI signal has less sensitivity to the displacement by one to two orders of magnitude. The transfer functions in Fig. 4. include the response of the EOMs and the photo detectors, and also phase delays due to the optical and signal paths after the photo detectors to the analyzer.

In Fig. 5, the orange dots are the simulated DFI response to a gravitational wave obtained by the measurement and computing, and the gray solid line is the DFI response predicted by Eq. (4). The response function of photo detectors, and of the mechanical resonance due to the EOM crystal, and the phase delays due to the optical paths and signal cables from beamsplitters to the analyzer are compensated properly in Fig. 5. The 3-D DFI response to a gravitational wave is well demonstrated around the peak frequency and its f^2 feature can be confirmed just below that frequency.

To summarize the results: we have successfully constructed and operated the 3-D DFI. The noise suppression feature of about 1 to 2 orders of magnitude and the retained DFI response were well simulated using EOMs over a wide frequency range.

We thank for Grant-in-Aid of the Japan Society for the Promotion of Science Fellows and Mitsubishi Foundation. This research is partially supported by the U.S. National Science Foundation.

[1] S. Kawamura and Y. Chen, *Phys. Rev. Lett.* **93**, 211103 (2004).
 [2] Y. Chen and S. Kawamura, *Phys. Rev. Lett.* **96**, 231102 (2006).
 [3] Y. Chen *et al.*, *Phys. Rev. Lett.* **97**, 151103 (2006).
 [4] S. Sato *et al.*, *Phys. Rev. Lett.* **98**, 141101 (2007).
 [5] S. P. Tarabrin and S. P. Vyatchanin, *Phys. Lett. A* **372**, 6801 (2007)

[6] A. A. Rakhubovsky and S. P. Vyatchanin, *Phys. Lett. A* **373**, 13 (2008)
 [7] K. Kokeyama, Ph.D. thesis, Ohanomizu University (2009)
 [8] We defined the output port whose path experiences transmission at the first beamsplitter and reflection at the second beamsplitter as the tr (transmission-reflection) port, and the other port as tt (transmission-transmission) port.